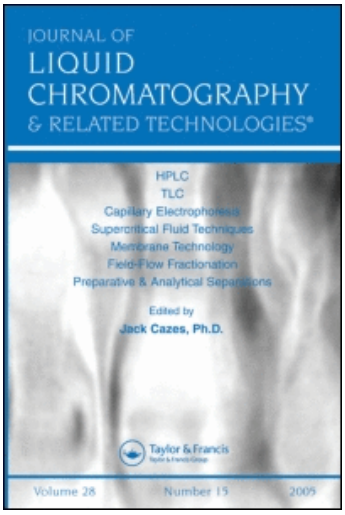

Journal of Liquid Chromatography & Related Technologies
Publication details, including instructions for authors and subscription information:
http://www.informaworld.com/smpp/title~content=t713597273

Inverse Optimal Filtering Method for the Instrumental Spreading Correction in Size Exclusion Chromatography

D. Alba[a]; G. R. Meira[a]
[a] INTEC (CONICET and Univ. Nac. del Litoral), Santa Fe, Argentina

To cite this Article Alba, D. and Meira, G. R.(1984) 'Inverse Optimal Filtering Method for the Instrumental Spreading Correction in Size Exclusion Chromatography', Journal of Liquid Chromatography & Related Technologies, 7: 14, 2833 — 2862
To link to this Article: DOI: 10.1080/01483918408067050
URL: http://dx.doi.org/10.1080/01483918408067050

JOURNAL OF LIQUID CHROMATOGRAPHY, 7(14), 2833-2862 (1984)

INVERSE OPTIMAL FILTERING METHOD FOR THE INSTRUMENTAL SPREADING CORRECTION IN SIZE EXCLUSION CHROMATOGRAPHY

D. Alba and G.R. Meira*
INTEC (CONICET and Univ. Nac. del Litoral)
(3000) Santa Fe, Argentina

ABSTRACT

The Kalman filter based techniques are adapted to solve the most general form of Tung's integral formula, i.e. when a non-uniform, non-symmetric calibration model is employed to correct chromatograms obtained in size exclusion chromatography from instrumental broadening errors. Through this method, the inverse smoothing of a chromatogram contaminated with measurement noise of known statistics is optimally performed by minimizing the estimation error variance. The method is numerically very "robust", improves the signal to noise ratio, provides good validation checks, and does not involve any previous parameter estimation procedure.

INTRODUCTION

Most of the methods of correction for instrumental broadening in size exclusion chromatography are based on the deterministic integral equation by Tung (1):

$$z(t) = \int_{-\infty}^{+\infty} u(\tau).g(t,\tau)\, d\tau \qquad (1)$$

where t,τ : both represent elution time or elution volume;
$z(t)$: is the baseline-corrected chromatogram;

(*) To whom correspondence should be sent.

 0148-3919/84/0714-2833$3.50/0

$g(t,\tau)$: is the unit mass (or normalized) detector response $g(t)$, for a truly monodisperse polymer species of retention time τ; and

$u(t)$: is the corrected chromatogram.

With different degrees of success, numerous techniques have been proposed for solving Eqn.(1), but most of them introduce one or both of the following simplifications into the instrumental spreading function:

a) $g(t,\tau)$ is adopted uniform, i.e. independent of the mean retention volume τ, e.g. (1,2,3,4,5,6,7); and

b) $g(t,\tau)$ is considered Gaussian, e.g. (8,9,10).

When the first simplification is adopted, the problem reduces to that of a deconvolution. In the case of the non-uniform Gaussian assumption, the variance is normally considered mean retention volume dependent. In some cases, e.g. (9,10), $u(t)$ is obtained not through a direct numerical solution of Eqn. (1), but after elaborate analytical procedures.

Among the few works that have attempted the direct solution of Eqn. (1) with no assumptions on $g(t,\tau)$ are those of Chang and Huang (11) and Ishige, Lee and Hamielec (12). According to a comparison of different techniques in (13,14), the best numerical method so far was that of (12).

The problem in hand is, in fact, a special case of the much more general one of input estimation or inverse filtering. Typically, a measurement signal must be corrected when the transducer frequency response is not flat over the whole signal frequency spectrum. For example, the inverse filtering of a ventricular pressure record is considered in (15); and the recuperation of seismic responses in oil prospection work is studied in (16, 17 and 18). In these last three publications, different adaptations of the Kalman filter (with or without smoother) were proposed and implemented to solve an inverse filtering problem.

In the present work, the feasibility of the use of inverse optimal smoothers for size exclusion chromatography broadening correction is demonstrated. The method has many characteristics in common with the mentioned works (16, 17 and 18). Nevertheless, it will be described here with some detail; with particular emphasis on the special features of the problem.

THEORY

The System Model

The application of the Kalman filter techniques requires a system description by means of a linear state-space stochastic model that, in our case, will adopt the following discrete single-input single-output form:

$$\underline{x}(k+1) = F(k)\ \underline{x}(k) + \underline{b}(k)\ w(k) \tag{2a}$$

$$z(k) = \underline{h}^T(k)\ \underline{x}(k) + v(k) = y(k) + v(k) \tag{2b}$$

where $k = 0,1,2,\ldots$: is the independent discrete time;

$\underline{x}(k)$: is the state vector;

$w(k)$ and $v(k)$: are zero-mean, Gaussian distributed white random sequences of variances $q(k)$ and $r(k)$, respectively;

$F(k)$: is, in general, a time-varying matrix; and

$\underline{b}(k), \underline{h}^T(k)$: are, in general, time-varying vectors.

The discrete stochastic version of Eqn. (1) can be written:

$$z(k) = \sum_{k_o=-\infty}^{+\infty} g(k,k_o).u(k_o) + v(k) \tag{3}$$

The time-varying calibration $g(k,k_o)$ can be considered as a set of discrete system impulse responses, with the impulses applied at times k_o. Note that in order not to introduce time shifts between the measured and the corrected chromatogram, the system must be assumed non-causal. This means that the response will start to appear before the application of the impulse, normally taken to occur at the maxima or at some mean value. Fig. 1a

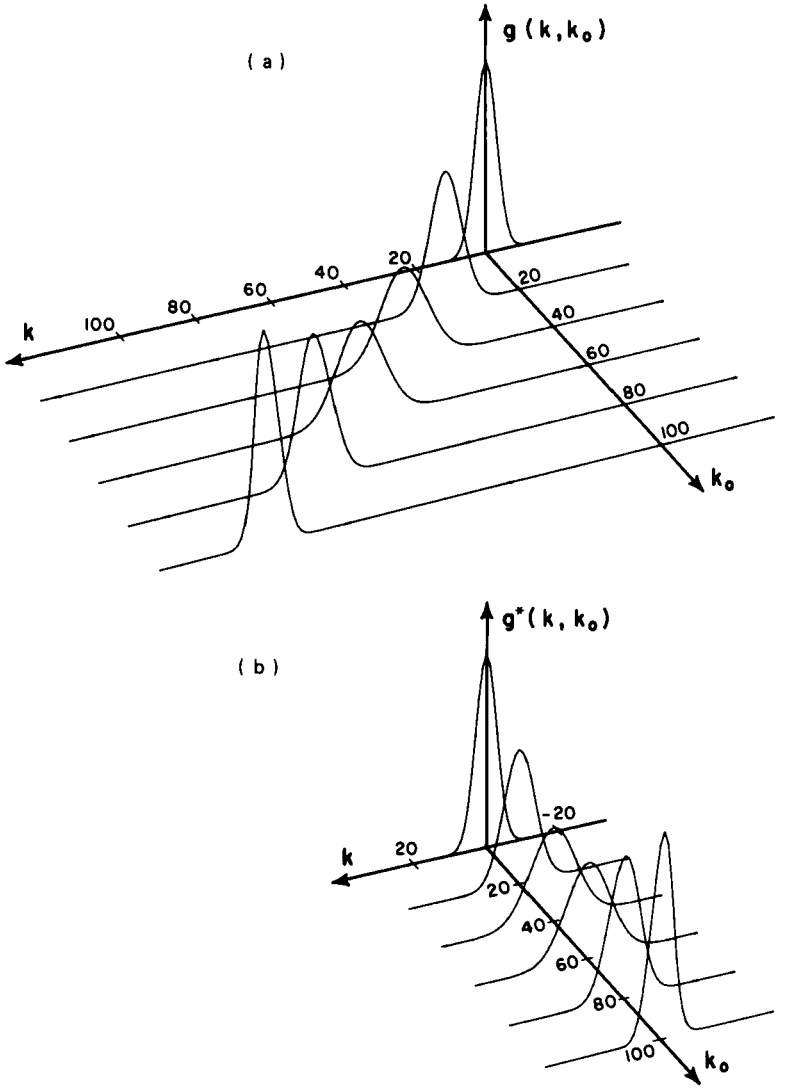

FIGURE 1 : A time-varying spreading function (a); and its corresponding g* function (b).

represents a time-varying impulse response, with the impulses applied at different k_o's . In what follows, it will be assumed that irrespective of k_o , all the responses have a finite number

of non-zero elements. Consider now some transformations to Eqn. (3) that will allow us to obtain the system state-space model in a straightforward fashion, and without calculations. As illustrated by Fig. 1b, let us first define the function $g^*(k,k_o)$, such that

$$g^*(k-k_o,k_o) = g(k,k_o) \tag{4}$$

Call -c and d the lower and upper limit of k with non-zero values of $g^*(k,k_o)$, respectively. Then Eqn. (3) yields:

$$z(k) = \sum_{k_o=k-c}^{k_o=k+d} g^*(k-k_o,k_o).u(k_o) + v(k) \tag{5}$$

and with $i=k-k_o$,

$$z(k) = \sum_{i=-c}^{d} g^*(i,k-i).u(k-i) + v(k) \tag{6}$$

The lower part of Fig. 2 shows a non-causal flow-diagram representation of Eqn. (6), where p^{-1} indicates the backshift operator such that $p^{-1}[u(k)] = u(k-1)$. The instantaneous set of weights g^* of Fig. 2 can be obtained from the successive row vectors $\underline{h}^T(k)$ of the following matrix H^*, where the rows $\underline{h}^T(k)$ extend at least to the calibration limits of the chromatographic column set.

$$H^* = \begin{bmatrix} . & . & \cdots & . & . \\ . & . & \cdots & . & g^*(-c,k-d) \\ . & . & \cdots & g^*(-c+1,k-d) & g^*(-c,k-d+1) \\ . & . & . & . & . \\ . & . & . & . & . \\ g^*(d,k-d-1) & g^*(d-1,k-d) & \cdots & g^*(-c+1,k+c-2) & g^*(-c,k+c-1) \\ g^*(d,k-d) & g^*(d-1,k-d+1) & \cdots & g^*(-c+1,k+c-1) & g^*(-c,k+c) \\ g^*(d,k-d+1) & g^*(d-1,k-d+2) & \cdots & g^*(-c+1,k+c) & g^*(-c,k+c+1) \\ . & . & & . & . \\ . & . & & . & . \end{bmatrix} \tag{7a}$$

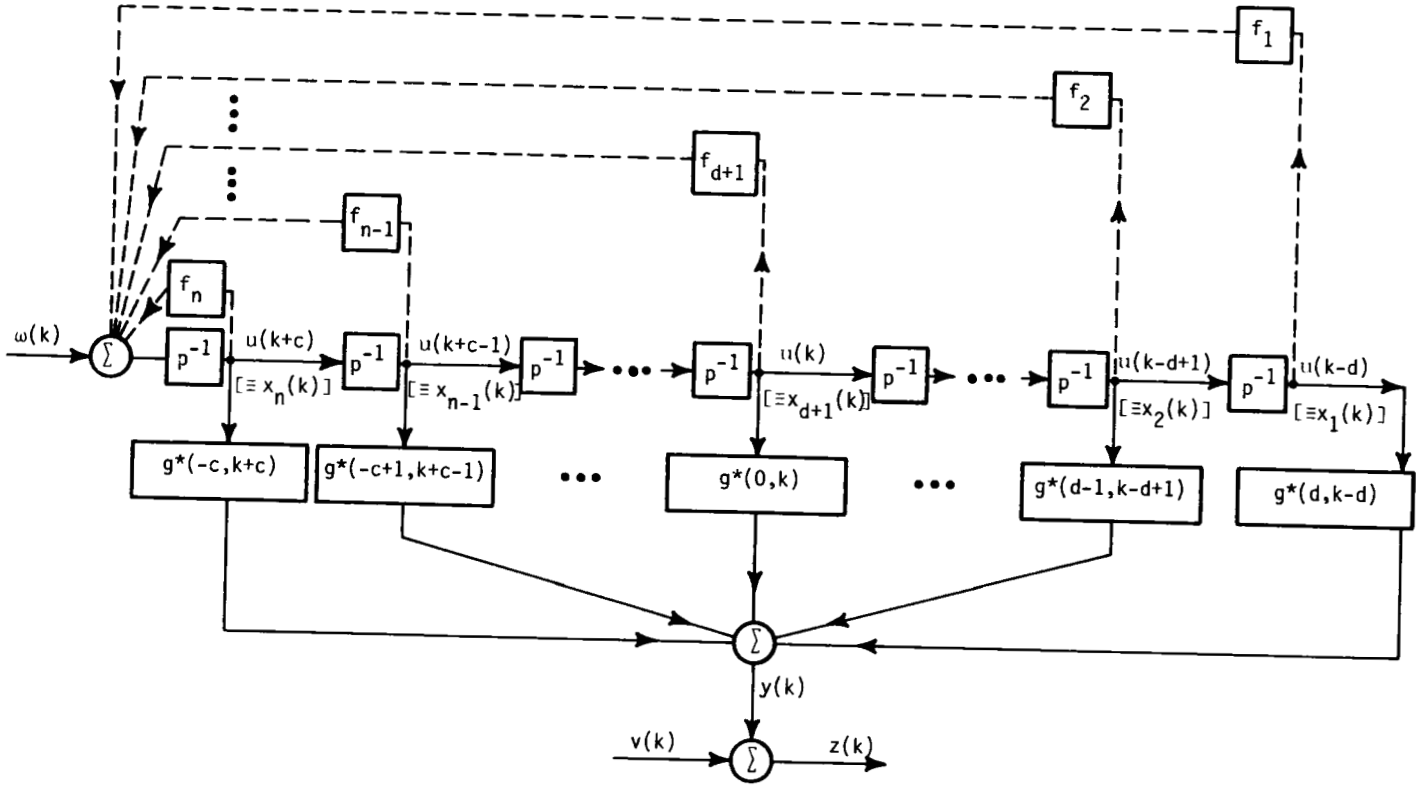

FIGURE 2 : System block-diagram from which the required state-space representation is obtained.

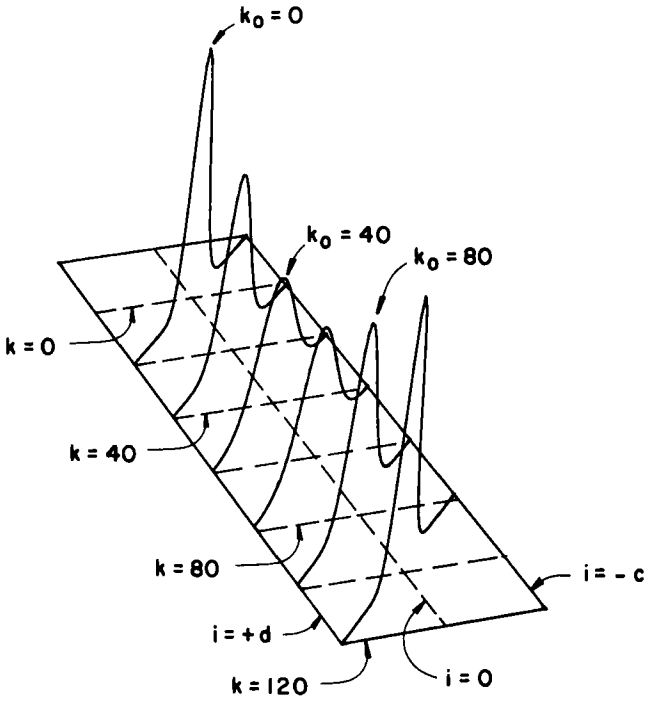

FIGURE 3 : H* matrix corresponding to the spreading function of Fig. 1, showing its 45° "diagonals".

or:

$$H^* = \begin{bmatrix} \vdots \\ \underline{h}^T(k-1) \\ \underline{h}^T(k) \\ \underline{h}^T(k+1) \\ \vdots \end{bmatrix} = \begin{bmatrix} \vdots & \vdots & & \vdots \\ h_1(k-1) & h_2(k-1) & \cdots & h_n(k-1) \\ h_1(k) & h_2(k) & \cdots & h_n(k) \\ h_1(k+1) & h_2(k+1) & \cdots & h_n(k+1) \\ \vdots & \vdots & & \vdots \end{bmatrix} \tag{7b}$$

Note that the successive 45° "diagonals" of H* are made up of the elements of the individual impulse responses. This is illustrated in Fig. 3. Let us define now $n = c+d+1$ state variables x_i $(i=1,\ldots,n)$ to coincide with the successive values of the in-

put, as indicated in Fig. 2. The system model output equation, which is equivalent to Eqn. (2b), may thus be written:

$$z(k) = \underline{h}^T(k).\underline{x}(k) + v(k) \qquad (8)$$

where $\underline{h}^T(k)$ is time-varying according to Eqn. (7).

The state equation itself allows the specification of the spectral characteristics that can be simultaneously assigned to all state variables, and consequently to $u(k)$ which coincides with $x_{d+1}(k)$. These spectral characteristics are imposed by filtering the white noise input $w(k)$ through an autoregressive operator, as indicated in the upper half of Fig. 2. Note that the order of this autoregressive operator is equal to the system order (which is normally relatively high). For this reason, a very satisfactory pre-filtering operation could, if desired, be implemented. The state equation, which is equivalent to Eqn. (2a), will have the following structure:

$$\begin{bmatrix} x_1(k+1) \\ x_2(k+1) \\ \vdots \\ x_{n-1}(k+1) \\ x_n(k+1) \end{bmatrix} = \begin{bmatrix} 0 & 1 & 0 & \cdots & 0 & 0 \\ 0 & 0 & 1 & \cdots & 0 & 0 \\ \vdots & \vdots & \vdots & & \vdots & \vdots \\ 0 & 0 & 0 & & 0 & 1 \\ f_1 & f_2 & f_3 & \cdots & f_{n-1} & f_n \end{bmatrix} \begin{bmatrix} x_1(k) \\ x_2(k) \\ \vdots \\ x_{n-1}(k) \\ x_n(k) \end{bmatrix} + \begin{bmatrix} 0 \\ 0 \\ \vdots \\ 0 \\ 1 \end{bmatrix} w(k) \qquad (9)$$

Note that matrices F and $\underline{b}$ are constant and in the controllable canonical form. The last row of F (that we shall call vector $\underline{f}$), allows the specification of the stated spectral characteristics of $u(k)$. When $\underline{f} = \underline{0}$, then $u(k)$ will be a white noise. The inclusion of non-zero elements in $\underline{f}$ will, in general, transform $u(k)$ into a "coloured" random sequence.

The Inverse Optimal Smoother

Under the assumption that the system is exactly represented by Eqns. (2), the "best" linear estimate of the state $\underline{x}(k)$ that

can be obtained from the noisy measurements $\{z(k) ; 0 < k < M\}$ is given by the output $\underline{\hat{x}}(k/M)$ of the optimal smoother. With $\underline{\hat{x}}(k/M)$ we shall indicate the "conditional estimate of $\underline{x}$ at time k given the measurements z up to time M". For general references see (19,20). The smoother is optimal in the sense that at each time k, the mean square error associated with the estimate $\underline{\hat{x}}(k/M)$:

$$E\{[\underline{x}(k) - \underline{\hat{x}}(k/M)]^T[\underline{x}(k) - \underline{\hat{x}}(k/M)]\}$$

is smaller than that achieved by any other linear estimator. Furthermore, if we also make the fairly common assumption that the initial state and the two random sequences satisfy Gaussian probability distributions, then the mean square error is less than that achieved by any other estimator, linear or non-linear. Fig. 4 illustrates the optimal smoother structure. The first stage corresponds to the Kalman filter and includes:

a) The discrete Riccati equation:

$$\Sigma(k+1/k) = F\ \Sigma(k/k)\ F^T + \underline{b}\ q(k)\ \underline{b}^T \tag{10a}$$

$$\Sigma(k/k) = \Sigma(k/k-1)\ \{ I - \underline{h}(k)\ [\underline{h}^T(k)\ \Sigma(k+1/k)\ \underline{h}(k) + r(k)]^{-1}\ \underline{h}^T(k)\ \Sigma^T(k/k-1)\} \tag{10b}$$

where: $\Sigma(k/k)$ is the estimation error covariance matrix, i.e.

$$\Sigma(k/k) = E\ \{[\underline{x}(k) - \underline{\hat{x}}(k/k)]\ [\underline{x}(k) - \underline{\hat{x}}(k/k)]^T\} \tag{10c}$$

b) The remaining algorithm:

$$\underline{g}(k+1) = \Sigma(k+1/k)\ \underline{h}(k+1)\ [\underline{h}^T(k+1)\ \Sigma(k+1/k)\ \underline{h}(k+1) + r(k+1)]^{-1} \tag{11a}$$

$$\tilde{z}(k+1) = z(k+1) - \underline{h}^T(k+1)\ F\ \underline{\hat{x}}(k/k) \tag{11b}$$

$$\underline{\hat{x}}(k+1/k+1) = F\ \underline{\hat{x}}(k/k) + \underline{g}(k+1)\ \tilde{z}(k+1) \tag{11c}$$

with

$$\underline{\hat{x}}(0/0) = \underline{\bar{x}}_o + P_o\ \underline{h}(0)\ [\underline{h}^T(0)\ P_o\ \underline{h}(0) + r(0)]^{-1}\ [z(0) - \underline{h}^T(0)\ \underline{\bar{x}}_o] \tag{11d}$$

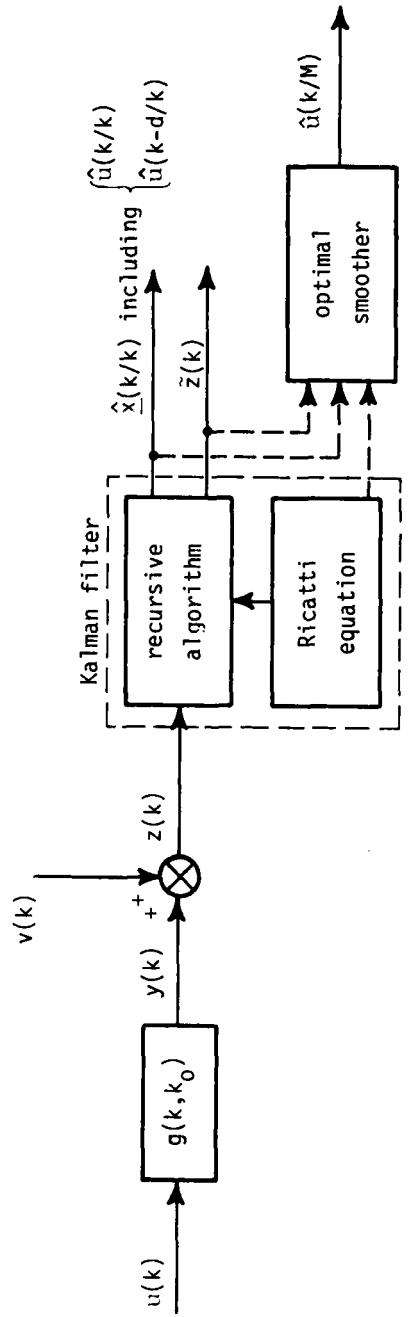

FIGURE 4 : Schematic representation of the optimal filter-smoother.

where: $\bar{x}_o$ and P_o : are the mean and covariance matrix of $\underline{x}(0)$, respectively;

$\underline{g}(k+1)$: is the filter gain; and

$\tilde{z}(k+1)$: is the innovations sequence.

In the second stage, the fixed-interval smoother algorithm taken from (19):

$$\underline{s}(k) = \underline{h}(k)\ r^{-1}(k)\ \underline{h}^T(k) \tag{12a}$$

$$\underline{\lambda}(k-1) = \left[I - \Sigma(k/k)\ \underline{s}(k)\right]^T \left[F^T(k)\ \underline{\lambda}(k) - \underline{h}(k)\ r^{-1}(k)\ \tilde{z}(k)\right] \tag{12b}$$

$$\hat{\underline{x}}(k/M) = \hat{\underline{x}}(k/k) - \Sigma(k/k)\ F^T(k)\ \underline{\lambda}(k) \tag{12c}$$

with

$$\underline{\lambda}(M) = \underline{0} \tag{12d}$$

is solved backwards in time.

Note that even though the filter section provides the estimate $\hat{\underline{x}}(k/k)$, and the smoother section the estimate $\hat{\underline{x}}(k/M)$, we are really only interested in the element (d+1) of these vectors, i.e.

$$\hat{x}_{d+1}(k/k) = \hat{u}(k/k) \tag{13a}$$

or

$$\hat{x}_{d+1}(k/M) = \hat{u}(k/M) \tag{13b}$$

Clearly, $\hat{u}(k/M)$ is a better estimate than $\hat{u}(k/k)$, but in the first case, a higher computational cost must be paid. The variance of the estimation error associated with $\hat{u}(k/k)$ is the element (d+1,d+1) of $\Sigma(k/k)$, and is automatically provided by the filter. The variance of the estimation error corresponding to $\hat{u}(k/M)$ must be especially calculated however [see (19)], but is always lower than that of the filter.

Because of the very special structure of the system model, the filter section inherently includes a suboptimal smoother: the so called fixed-lag smoother. In fact, if this lag is limited to

d, a suboptimal estimate (better than $\hat{u}(k/k)$) is produced, without extra calculations. In effect, since

$$x_1(k+d) = x_2(k+d-1) = \ldots = x_d(k+1) = x_{d+1}(k) \tag{14}$$

then,

$$\hat{x}_1(k+d/k+d) = \hat{x}_{d+1}(k/k+d) \tag{15}$$

and therefore,

$$\hat{x}_1(k+d/k+d) = \hat{u}(k/k+d) \tag{16}$$

In other words, the filter estimate $\hat{x}_1(k+d/k+d)$ is the fixed-lag smoothed estimate of $u(k)$, and the corresponding estimation error variance is element (1,1) of $\Sigma(k+d/k+d)$. Note also that by artificially increasing the system dimension n (with an appropriate inclusion of zeroes on the left hand side of matrix H^*), the suboptimal smoother lag is also increased. When $c > d$, the lag can be increased to c by filtering $z(k)$ backwards in time.

The Algorithm Adjustment

The following parameters must be set in the given algorithm:

a) *The last row of matrix F (row vector $\underline{f}$)*

Only two cases will be considered: $\underline{f} = \underline{0}$ and $\underline{f} = (0\ 0 \ldots 1)$. In the first case, $u(k)$ is assumed a white noise process; in the second a "random walk" process. By assuming $u(k)$ a white noise, the greatest flexibility in its estimation is provided; and one could, for example, recuperate delta functions when analyzing monodisperse samples. When a polidisperse sample is analyzed, then a smoothing effect (that in general improves the numerical results) may be obtained if $u(k)$ is considered a random walk. As explained below, the other advantage of assuming $\underline{f} = (0\ 0 \ldots 1)$ is related to the mean of the innovations sequence.

b) *The initial conditions $\overline{\underline{x}}_o$ and P_o*

In practice, it has been found adequate to choose $\overline{\underline{x}}_o = \underline{0}$ and $P_o = I$; and to solve the Riccati equation with $\underline{h}^T(0)$ until

steady state conditions are reached. Then, the chromatogram above the baseline may be directly processed. In the examples of the following section, this procedure was adopted in all cases.

c) *The measurement noise variance r(k)*

This value can be estimated from the noise that normally contaminates the detector baseline before and after the polymer peak. It will be hereafter considered constant, of value r.

d) *The input variance q(k)*

Consider first some ways of estimating $q(k)$ when $\underline{f} = \underline{0}$. In this case, the state variables are assumed white processes with a variance:

$$\sigma^2_{x_{i(k)}} = q(k-n-1+i) \quad ; \quad (i = 1,2,\ldots,n) \tag{18}$$

($\sigma_{a(k)}$ will denote the variance of $a(k)$, and $\bar{a}(k)$ its mean value). It is also easy to show that:

$$\sigma^2_{z(k)} = \sum_{i=1}^{n} h_i^2(k)\, q(k-n-1+i) + r \tag{19}$$

Eqn. (19) has no solution because $\sigma^2_{z(k)}$ is unknown. Even if this function could be estimated, Eqn. (19) is of the same type of Eqn. (3) (which we are trying to solve), and therefore is still of no practical use unless some simplifications are added. The simplest situation is to consider $w(k)$ stationary, and the spreading function uniform. Under these circumstances, an estimate for a constant value of q may be obtained from Eqn. (19) as follows:

$$q = \frac{\sigma^2_z - r}{\sum_{i=1}^{n} h_i^2} \tag{20a}$$

with

$$\sigma^2_z = \frac{\sum_{i=1}^{M} [z(k)]^2}{(M-1)} \tag{20b}$$

Eqn. (20) in general overestimates q because $u(k)$ is a highly correlated sequence instead of a white noise. Nevertheless, Eqn. (20) may provide an initial guess of q that can be useful if properly handled. In case of a non-uniform spreading function, the denominator of Eqn. (20a) could correspond to the impulse response at an intermediate retention time.

Consider now $w(k)$ non-stationary (i.e. q variable with k). This assumption has been found essential for particularly ill-conditioned cases. In fact, if r is accurately estimated, the optimal performance of the filter-smoother is produced when the exact $q(k)$ is utilized. Note that $\underline{f} = \underline{0}$ implies $w(k) = u(k+c+1)$. Thus, if $u(k+c+1)$ can be somehow estimated, then one may simply write

$$q(k) = \left[\hat{u}(k+c+1)\right]^2 \tag{21}$$

For example, $\hat{u}(k+c+1)$ in Eqn. (21) could be the smoother solution obtained with a constant q. Alternatively, the following approximate formula (that may be also derived from Eqn. (19) assuming no spreading), has been found to provide satisfactory results:

$$q(k) = C\left[z(k+c+1)\right]^2 \tag{22}$$

where C is an appropriately chosen positive constant. For $C = 1$, $q(k)$ will be, in principle, underestimated for $u(k) < z(k)$ and overestimated when $u(k) > z(k)$. The estimates of $q(k)$ based on Eqns. (21) or (22) have little statistical significance because they are obtained from single values of $u(k+c+1)$ or $z(k+c+1)$. This means that sudden changes in these functions will be reflected on the estimate $q(k)$. A simple remedy is to smooth $u(k+c+1)$ or $z(k+c+1)$ through an averaging filter in order to keep the shape of these curves while eliminating the undesirable variations.

Consider now the estimation of $q(k)$ when $\underline{f} = (0\ 0 \ldots 1)$. It may be shown that when $w(k)$ is assumed stationary, the equivalent formula to Eqn. (20) is:

$$q = \frac{\sigma^2_{\Delta z(k)} - 2r}{\sum_{i=1}^{n} h_i^2} \tag{23a}$$

with

$$\sigma^2_{\Delta z(k)} = \frac{\sum_{i=1}^{M} [\Delta z(k)]^2}{(M-1)} \tag{23b}$$

A simple expression for $q(k)$ can be developed from the fact that $w(k) = u(k+c+1) - u(k+c) = \Delta u(k+c+1)$, and therefore:

$$q(k) = [\Delta\hat{u}(k+c+1)]^2 \tag{24}$$

For the reasons given above, but particularly in this case, it is preferable to employ averaged versions of $\Delta\hat{u}^2$ instead of $\Delta\hat{u}^2$ as such. The following equation was found adequate:

$$q(k) = C' \frac{\sum_{i=-a}^{a} [\Delta\hat{u}(k+c+1+i)]^2}{(2a+1)} \tag{25}$$

where C' is an adjustable gain and $(2a+1)$ is the number of points averaged at each step. Clearly, here again, an iterative procedure that estimates $q(k)$ from $\Delta\hat{u}(k)$, and then $\hat{u}(k)$ and $\Delta\hat{u}(k)$ from the filter-smoother, will normally provide the best results. The results of the filter-smoother are not too sensitive to its adjustment, and relatively crude estimates of the shape of $q(k)$ are normally sufficient for satisfactory results. For example, in certain cases, Eqn. (25) provides a smooth $q(k)$, with a shape which is similar to that of $z(k)$. In such cases, and even when $\underline{f} = (0\ 0 \ldots 1)$, an estimate of $q(k)$ may be directly obtained from the simpler relationship of Eqn. (22). This simplification is conveniently utilized in Examples 2 and 3 below.

Even though the covariance matrices $\Sigma(k/k-1)$ and $\Sigma(k/k)$ depend on the individual values of r and $q(k)$, the filter or

the smoother estimate of $u(k)$ is a function of the $q(k)/r$ ratio only. In a very ill-conditioned problem, the results become sensitive to deviations of this ratio from its correct value. In more relaxed situations however, relative gross errors in $q(k)/r$ can be absorbed with still good results.

The solution validation

The solution checks may be classified into two main groups: those which are common to any other input estimation technique, and those specific to the method. The obvious checks in the first group are: a) the solution must be non-negative; b) by processing $\hat{u}(k)$ through the system spreading function, the noise-free measured function should be recuperated; and c) the area under the corrected chromatogram must be equal to that of the measured curve. It should be emphasized that the check under b) is only a necessary (but not a sufficient) condition for good results; the reason being the algorithmic singularity of Eqns. (1) or (3). This implies that there are, in principle, infinite possible numerical solutions $\hat{u}(k)$ that can recover $y(k)$. With regards to the check under c), the area under the corrected curve will be smaller than that of the original, only when the ratio $q(k)/r$ is grossly undervalued. With overvalues or moderate undervalues of $q(k)/r$, then numerically meaningless discrepancies are observed.

The checks which are specific to the method are all based on the analysis of the innovations, that ideally should be zero-mean, Gaussian white sequences. Furthermore, the observed innovations should match the corresponding time-varying variance estimated through the filter:

$$\sigma^2_{\tilde{z}(k)} = \underline{h}^T(k)\ \Sigma(k/k-1)\ \underline{h}(k) + r \qquad (26)$$

Note that this last quantity depends again on the individual values of $q(k)$ and r. The filter results may be optimized by analyzing the innovations (and their estimated variances) under different adjustments. The innovations mean will, in general, be closer to zero with $\underline{f} = (0\ 0 \ldots 1)$ than with $\underline{f} = \underline{0}$. This may be

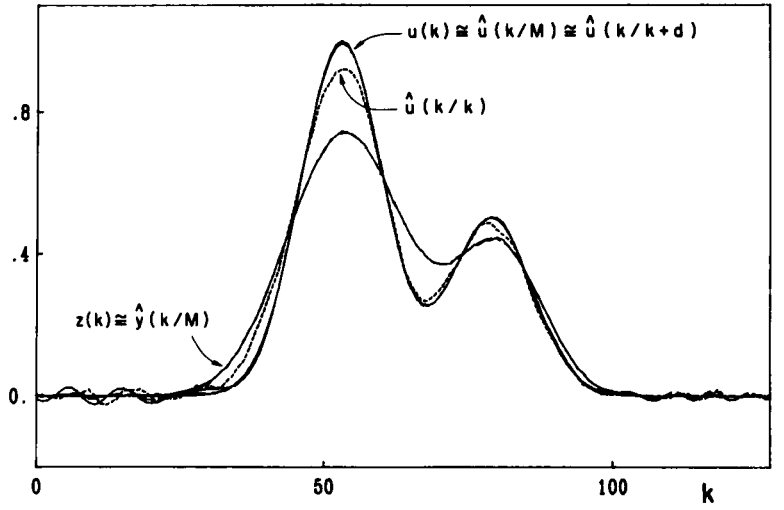

FIGURE 5 : Example 1; original curves and "best" solution with the correct constant ratio q/r = 100.

explained by the offset elimination effect that occurs when integration is incorporated into a closed loop.

EXAMPLES OF APPLICATION

Three applications of the technique will be considered. While the first two examples are synthetic, the third is based on real experimental data. All three examples were solved by means of a VAX 11/780 computer.

Example 1

By processing the curve u(k) shown in Fig. 5 through a time-varying filter defined by the set of impulse responses of Fig. 1a, a noise-free chromatogram y(k) is obtained. This curve was then corrupted by a Gaussian white noise of a relatively low variance (10^{-5}), to provide z(k). Taking into account only the section of this series above the baseline, and defining the signal to noise ratio SNR as:

$$SNR = \frac{\sum_{k=1}^{M} z^2(k)}{(M-1)\,r} \tag{27}$$

one obtains, in this case, $SNR \cong 17400 \cong 132^2$. Throughout this Example $\underline{f} = (0\ 0 \ldots 1)$, and for simplicity a constant q will be adopted even though better results can, in principle, be obtained with a variable $q(k)$. Clearly, the best estimate for r is 10^{-5}. The best estimate of q may be obtained from:

$$q = \frac{1}{(M-1)} \sum_{k=1}^{M} [\Delta u(k)]^2 \tag{28}$$

Calculating this quantity for the $\Delta u(k)$ values above the baseline, 0.001 is obtained. Thus, the best q/r is 100. Note that if estimated through Eqn. (23), a value of q approximately 10-fold larger would have been obtained. The results of the filter-smoother when the best values for q and r are adopted are also shown in Fig. 5. While the filter estimate $\hat{u}(k/k)$ fails to reproduce the original curve, both the fixed-lag smoother output $\hat{u}(k/k+d)$ and the fixed-interval smoother output $\hat{u}(k/M)$ are practically overlapped with $u(k)$. The innovations corresponding to this case are represented in Fig. 6d, together with the estimated $\pm\sigma_{\tilde{z}(k)}$ limits. Ideally, the innovations should lie within these limits for approximately two thirds of the time, and this is roughly the case in Fig. 6d. The innovations sequence $\tilde{z}(k)$ is theoretically zero-mean Gaussian white, but its variance is time-varying and therefore $\tilde{z}(k)$ is non-stationary. In spite of this fact, it was found useful to calculate the sequence sample variance $\sigma^2_{\tilde{z}}$, the autocorrelation function and the power spectrum. Clearly, this approximation will not be valid when $\tilde{z}(k)$ is highly non-stationary. Figs. 6e and f illustrate the previously mentioned statistics. In the case of the power spectrum, the highest frequency shown corresponds to one half of the sampling frequency. Both the autocorrelation and the power spectrum show some low fre-

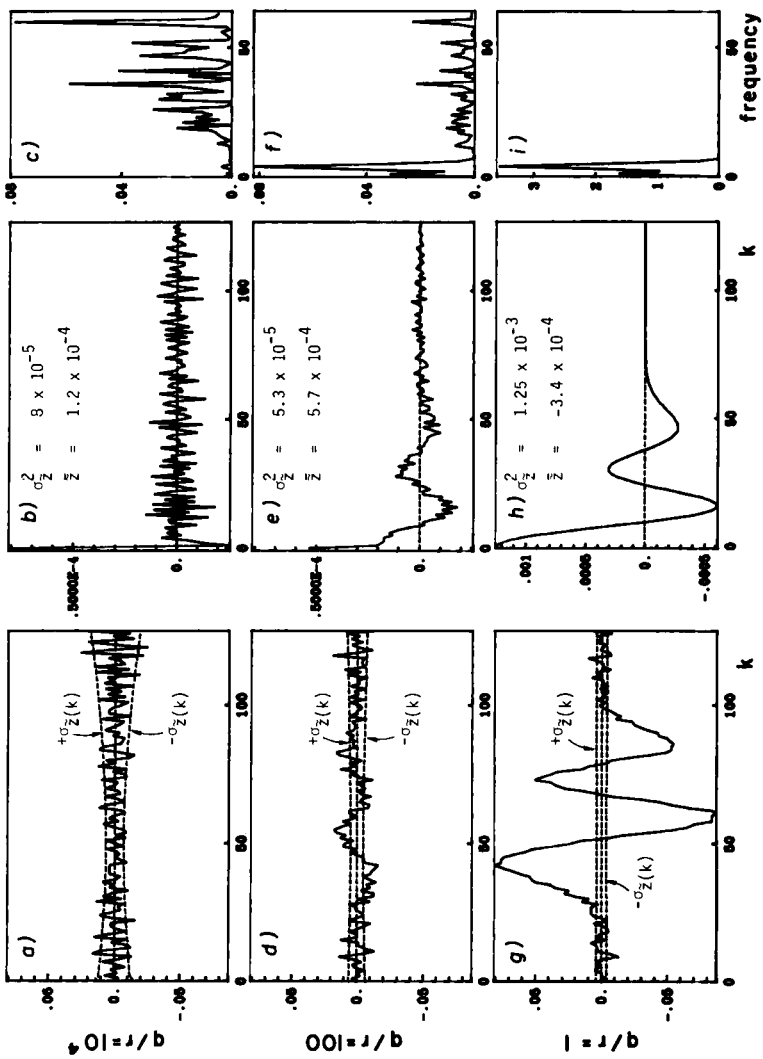

FIGURE 6 : Example 1; Innovations analysis corresponding to an overvalued q/r ratio (a,b,c), to the correct q/r ratio (d,e,f) and to an undervalued q/r ratio (g,h,i).

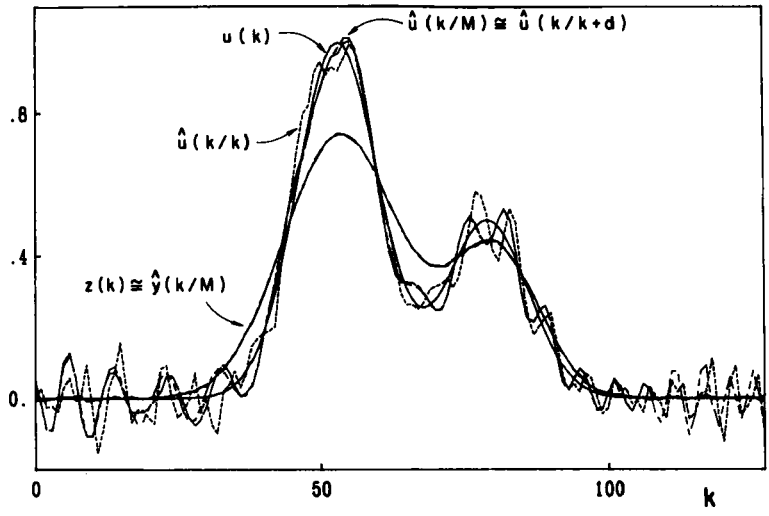

FIGURE 7 : Example 1; solution for $q/r = 10^4$.

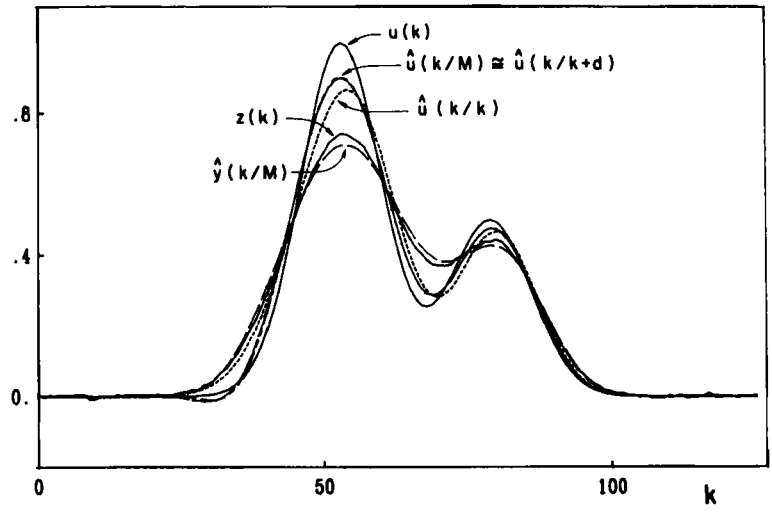

FIGURE 8 : Example 1; solution for $q/r = 1$.

quency oscillations. This, and the fact that the smoother estimate is satisfactory while the filter estimate is not indicate that some useful information is still remaining in the innovations sequence.

For illustrative purposes, the problem was solved again with the same value of r, but with erroneous estimates of q. In Figs. 7, 6a, 6b, and 6c, $q = 0.1$ (or $q/r = 10000$), while in Figs. 8, 6g, 6h, and 6i, $q = 10^{-5}$ (or $q/r = 1$). Note the following:

i) In both cases, the solutions are inadequate, but while $y(k/M)$ practically coincides with $z(k)$ when $q = 0.1$, this same function is crudely off those values if $q = 10^{-5}$.

ii) When q is overvalued, the innovations are less correlated at high lags than if the best value of q is employed. The opposite occurs at low lags however, and the overall variance of $\tilde{z}(k)$ is finally higher than before. If q is under valued, the situation is clearly worse at all lags.

iii) The standard deviation $\sigma_{\tilde{z}(k)}$ is overestimated if q is overvalued, and underestimated when undervalued.

iv) The high frequency components of the innovations are dominant if q is overestimated. Conversely, there is a low frequency components dominance when q is underestimated.

v) The percentages of variation of the areas under the corrected chromatograms with respect to those under the measured curves are -0.02%, -0.1% and -0.25% when $q = 0.1$, 0.001 and 10^{-5}, respectively.

Example 2

This Example was first suggested by Chang and Huang (6), and attempted later on by Hamielec and co-workers (12). The problem is illustrated in Fig. 9, which represents the following: $u(k)$, the uniform spreading function $g(k)$, the broadened curve $z(k)$ and the recuperated $u(k)$ by method 2 proposed in (12). Note that while $g(k)$ was generated from an analytical expression, and $z(k)$

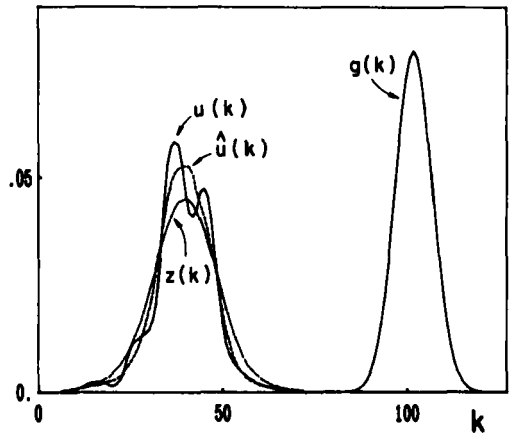

FIGURE 9 : Example 2; [after Hamielec and co-workers (12)].

was reproduced from a table of numbers given in (12), u(k) and u(k) were obtained by digitizing their graphical representations. For this reason, minor distorsions in these last two curves are to be expected. The solution $\hat{u}(k)$ shown in Fig 9 is practically coincident with that of (6), and with that of method 1 in (12). Clearly, these techniques are not able to appropriately recover the double-peaked input.

Consider now the solution via the present method. Assuming that the integer values of the table for z(k) are all accurate to the last digit, then one may interpret those numbers as contaminated by a noise v(k) of a uniform probability density function with limits at ±0.5. In this case, $\sigma_v^2 = 1/12$ and we adopt $r = 0.1$. The limits of the finite spreading function were taken at $-c = d = 20$. Beyond these values, the spreading function is below 10^{-3} .

As a first attempt, one could try to solve this Example through a constant q obtained by minimizing the variance of the innovations sequence. The solution $\hat{u}(k/M)$ is not shown here, but is very similar to that of Fig. 9, however. For better results, a variable q(k) must be adopted, and Fig. 10 illustrates this sit-

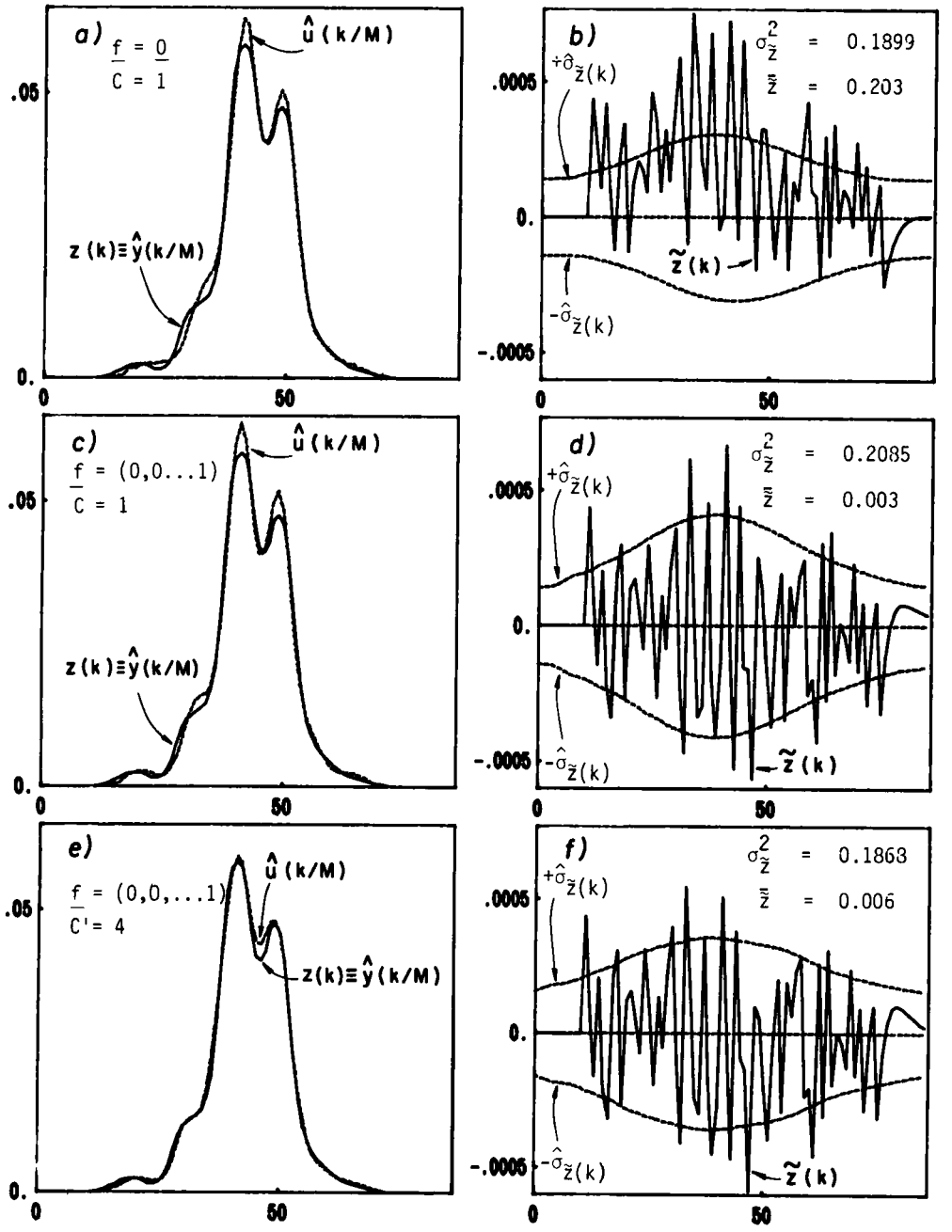

FIGURE 10 : Example 2; solutions considering u(k) white (a,b); considering u(k) a random walk sequence (c,d); and obtained through a two-step procedure (e,f).

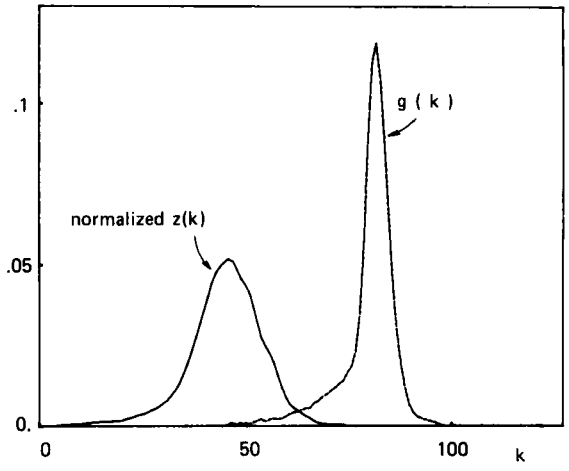

FIGURE 11 : Example 3; experimental chromatogram and spreading function.

uation. Note first that (even though not shown), all three solutions represented in Fig. 10, as well as that previously mentioned with a constant q, manage to recuperate z(k) without appreciable error.

The solution of Fig. 10a and 10b was obtained adopting $\underline{f} = \underline{0}$ and calculating q(k) through Eqn. (22) with C = 1. Clearly, the peaks of $\hat{u}(k/M)$ overpass those of u(k), and the innovations mean exhibits a certain bias. In Figs. 10c and 10d, Eqn. (22) is used again (with C = 1), in spite of the fact that in this case, $\underline{f}$ = (0 0...1). The result is similar to the previous, but now the innovations mean is very close to zero. Figs 10e and 10f were obtained through the following two-step procedure: i) based on the estimate of u(k) found in Fig. 10a, Eqn. (25) with C' = 4 was employed to estimate q(k); and ii) with this estimate, the smoother was run again with $\underline{f}$ = (0 0...1) to provide the shown results. Clearly, this solution is very acceptable. The corresponding innovations have a near zero mean, and the lowest sample variance of all three cases.

Example 3

Curve $z(k)$ in Fig. 11 represents the chromatogram of a PS standard of molecular weight $M_w = 525$, when fractionated through an A-802 Shodex column mounted on a Series 3-B Perkin Elmer liquid chromatograph. The chromatogram of pure benzene $g(k)$ is adopted as the uniform spreading function. The polymer sample is expected to be integrated by the first PS oligomers, with preponderance of the pentamer. Ideally therefore, delta functions ought to be recuperated, with the highest peak at a molecular weight of 520.

Three possible solutions to this problem are found in Fig. 12. In all three cases, the solutions accurately recuperate the measured chromatogram, r was estimated 5×10^{-5} and $q(k)$ was obtained through Eqn. (22). Figs. 12a and 12b show a quite acceptable solution, where all oligomers from dimer to hexamer are now clearly separated. The adjustments employed in this first solution are: $\underline{f} = \underline{0}$, and a C gain of 1.25 for Eqn. (22).

With C gains higher than 1.25, negative values in $\hat{u}(k/M)$ are produced. This situation is represented by Figs. 12c and d, where $\underline{f} = \underline{0}$ but $C = 75$. This value of C will clearly generate an overestimated $q(k)$. In this case, and in spite of the negative values in $\hat{u}(k/M)$, the low molecular weight peaks appear to be better separated, and two extra higher molecular weight components seem to be also detected. The innovations sample mean and variance indicated in Fig. 12d are lower than in Fig. 12b, but the estimated $\pm\sigma_{\tilde{z}(k)}$ limits confirm that this solution is not adequate.

Figs. 12e and f show a solution which is very similar to that of Figs. 12a and b; but in this case $\underline{f} = (0\ 0 \ldots 1)$ and $C = 2$ were adopted. Here again, by increasing C, negative values are also produced.

The estimates of Figs. 12a and 12e are the best obtained. The oligomers are clearly separated, and their retention times could be used for a more accurate column calibration. As expected, those retention times are, with good approximation, linearly re-

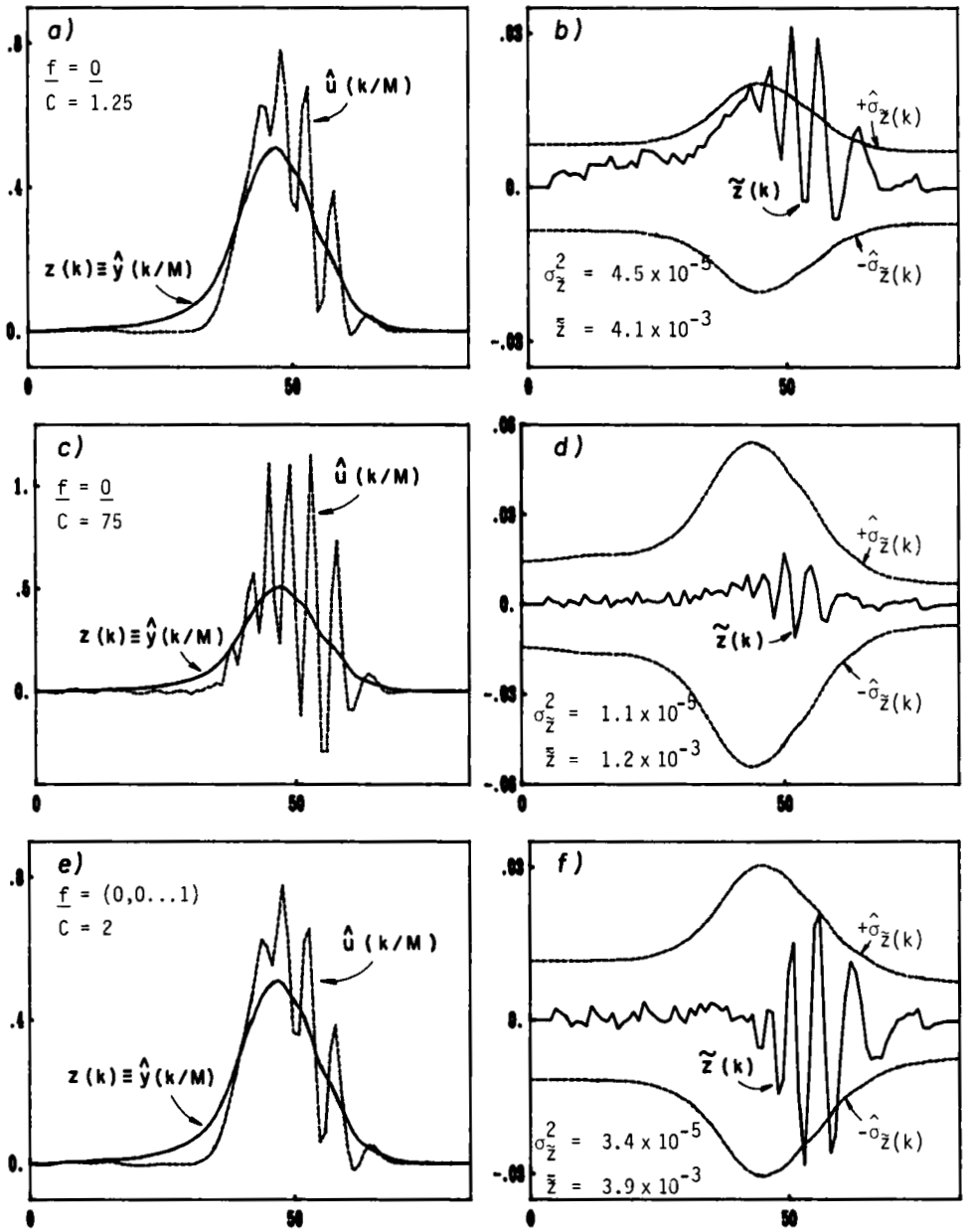

FIGURE 12 : Example 3; solutions considering u(k) white with the appropriate C gain (a,b); with C overvalued (c,d); and considering u(k) a random walk sequence with the appropriate C (e,f).

lated to the logarithm of their molecular weights.

The results of Fig. 12 seem to indicate that the lower molecular weight species are better separated than the higher. This bias is also reflected by the fact that in all cases, the innovations adequately match their $\pm\sigma_{\tilde{z}(k)}$ limits only on the right hand side of the chromatogram. A possible explanation to this effect is that the spreading function is, in reality, non-uniform. In this case, the given $g(k)$ is only accurate at the low molecular weight end. If as predicted by (21,22), the instrumental broadening increased towards intermediate retention volumes, then the correction would be more pronounced on the left hand side of the curve, and the bias would tend to be compensated.

CONCLUSIONS

The proposed technique has proved very powerful with both synthetic and real examples, and could be clearly extended to corrections in hydrodynamic chromatography (13,14). The results of Example 2, are better than those of other techniques. The computer program was written in FORTRAN 77 for a VAX 11/780 computer, and is available from the authors.

The main advantages of the method are: i) it is numerically very 'robust', thus allowing the solution of particularly ill-conditioned problems; ii) because a stochastic version of Eqn. (1) is employed, all 'a priori' information on the baseline noise may be conveniently employed; iii) under certain ideallized conditions, the solution is optimal from the standpoint of the estimation error variance; iv) the state-space representation of the system spreading function is obtained without calculations, thus involving no assumptions about the shapes of the calibration curves; v) the innovations analysis provides very powerful solution checks, and vi) the measurement noise is eliminated from the corrected chromatogram and the SNR of $y(k)$ is normally higher than that of $z(k)$.

The main drawback of the method deals with the relatively significant computational cost involved. With regards to memory, not only the system matrix H^* and the measured and calculated sequences must be stored, but (more important) the whole set of matrices $\Sigma(k/k)$. The computation time is also relatively high. For example, to solve an 80 point chromatogram with a calibration curve of 55 points (Example 3 above), approximately 12 minutes are required for the complete calculation, with half that time insumed in the fixed-interval smoother stage. The computation time increases with approximately the square of the system order n; and in the Kalman filter section, the main computational burden is related to the solution of the discrete Riccati equation. Note that if the same calibration $g(k,k_o)$ is to be repeatedly used, and the variances q and r are maintained constant, then this equation may be solved only once. Furthermore, when q and r are constant and the spreading function is uniform, then only the steady state solution of that equation is required.

In all cases considered, the results of the fixed-lag smoother when the lag was made equal to c or d were very similar to those of the fixed-interval smoother. Clearly, if the fixed-lag smoother results are adequate, not only the computation time is approximately halved, but also the storage of the covariance matrices set is no longer required.

In this work, the state variables [and consequently $u(k)$] were assumed white processes if $\underline{f} = \underline{0}$, and random walk processes when $\underline{f} = (0\ 0 \ldots 1)$. Both assumptions were seen to provide satisfactory results, but the innovations mean was in all cases smaller with $\underline{f} = (0\ 0 \ldots 1)$. As a counterpart in this last case, the estimation of $q(k)$ becomes more complex. Theoretically, the best results would require a specification of vector $\underline{f}$ that included all available information about $u(k)$. This was found not necessary in the processing of chromatograms, but in a different context, interesting efforts have been done in this direction although mainly dealing with time-invariant systems (23,24). In a

way, an appropriate estimation of $q(k)$ compensates a rather crude estimation of $\underline{f}$.

As explained above, the main advantage of the state-space time-varying model proposed is that no calculations for its development are required. The high order of the model so produced, makes the smoother computation a relatively arduous task, however. Alternatively, parameter estimation procedures could be employed to identify the system through lower order models. This identification stage could be implemented off-line, and then repeatedly used for a given calibration. Another potential advantage of this procedure is the elimination of the measurement noise from the set of curves $g(k,k_o)$; while the main disadvantage is that elaborate identification procedures for time-varying systems are not yet fully developed. The other possible modification to the proposed technique deals with the implementation of a variable gain scheme for an on-line estimation of $q(k)$ (25). Basically, the problem consists in choosing, along the calculation, the values of $q(k)$ which minimize the difference between the observed and the estimated innovations variance.

ACKNOWLEDGEMENTS

To CONICET and to the Univ. Nac. del Litoral for the financial support. To Mr. M. Brandolini for his invaluable help with the experiments and with the software development.

REFERENCES

1) Tung, L.H., J. Appl. Polym. Sci., 10, 375 (1966).

2) Balke, S.T. and Hamielec, A.E., J. Appl. Polym. Sci., 13, 1381 (1969).

3) Pierce, P.E. and Armonas, J.E., J. Polym. Sci. C, 21, 23 (1968).

4) Tung, L.H., J. Appl. Polym. Sci., 13, 775 (1969).

5) Tung, L.H., J. Appl. Polym. Sci., 10, 1271 (1966).

6) Chang, K.S. and Huang, Y.M., J. Appl. Polym. Sci., 13, 1459 (1969).

7) Alba, D. and Meira, G.R., J. Liq. Chromatogr., 6(13), 2411 (1983).

8) Vozka, S. and Kubin, M., J. Chromatogr., 139, 225 (1977).

9) Hamielec, A.E., J. Liq. Chromatogr., 3(3), 381 (1980).

10) Hamielec, A.E., Ederer, H.J. and Ebert, K.H., J. Liq. Chromatogr., 4(10), 1697 (1981).

11) Chang, K.S. and Huang, Y.M., J. Appl. Polym. Sci., 16, 329 (1972).

12) Ishige, T., Lee, S.-I. and Hamielec A.E., J. Appl. Polym. Sci., 15, 1607 (1971).

13) Penlidis, A., Hamielec, A.E. and MacGregor, J.F., J. Liq. Chromatogr., 6(S-2), 179 (1983).

14) Silebi, C.A. and McHugh, A.J., J. Appl. Polym. Sci., 23, 1699 (1979).

15) Demoment, G., 'Algorithme de Deconvolution ...', Proc. of "Journess d'etude sur la deconvolution des signaux", CEN Cadarache (1982).

16) Bayless, J.W. and Brigham, E.O., Geophysics, 35(1), 2 (1970).

17) Crump, N., Geophysics, 39(1), 1 (1974).

18) Mendel, J.M., IEEE Trans. Geosci. Remote Sensing, GE-19(3) (1981).

19) Bryson, A.E. and Ho, Y.-C., 'Applied Optimal Control', John Wiley & Sons (1975).

20) Anderson, B.D.O. and Moore, J.B., 'Optimal Filtering', Prentice Hall (1979).

21) Tung, L.H. and Runyon, J.R., J. Appl. Polym. Sci., 13, 2397 (1969).

22) Gao, Y.-S., Ye, M.-L., Le, H.-J., Ding, Y.-K., Ying, Q.-C. and Sang, M.-M., J. Liq. Chromatogr., 5(7), 1241 (1982).

23) Young, P. C. and Jakeman A. J., CRES Report AS/R28 Australian National University, Canberra ACT (1979).

24) Ahlen, A., UPTEC 8450R, Teknikum Institute of Technology, Uppsala University, Sweden (May 1984).

25) Jazwinski, A.H., 'Stochastic Processes and Filtering Theory', Academic Press (1970).